Comparative Study of Ultrasound Stimulation and Conventional Heating Methods on the Preparation of Nanosized γ-Al_2O_3

Abhijit Majhi,[†] G. Pugazhenthi,*[,†] and Anupam Shukla[‡]

Department of Chemical Engineering, Indian Institute of Technology Guwahati, Guwahati, 781039, India, and Department of Chemical Engineering, Indian Institute of Technology Delhi, New Delhi, 110016, India

This work addresses the advantages of the ultrasound stimulation method over the conventional heating method for the preparation of nanosized γ-Al_2O_3. The γ-Al_2O_3 obtained by calcination of boehmite at 600 °C is derived from the inexpensive aluminum chloride salt by the precipitation route. Thermal evolution, phase transformation, surface area, and particle size distribution of the boehmite and γ-Al_2O_3 are characterized by thermogravimetric analysis (TGA), X-ray diffraction (XRD), Fourier transform infrared analysis (FT-IR), nitrogen adsorption−desorption isothermal data, and dynamic light scattering analysis (DLS). The γ-Al_2O_3 prepared by ultrasound stimulation has higher surface area (256 $m^2\ g^{-1}$), bigger pore diameter (6.06 nm) and larger cumulative pore volume (0.388 $cm^3\ g^{-1}$) than the conventional heating method (surface area, pore diameter, and pore volume of 219 $m^2\ g^{-1}$, 5.61 nm, 0.307 $cm^3\ g^{-1}$, respectively), which are even higher than the value reported in the literature for γ-Al_2O_3 synthesized at 100 °C for 24 h aging (pore diameter of 4.27 nm and pore volume of 0.26 $cm^3\ g^{-1}$). The sonication applied during the aging of boehmite sol reduces the crystallite size (or particle size) and increases the porosity. The boehmite and γ-Al_2O_3 obtained by sonication have the highest porosity of 46% and 59%, respectively, without using any structure directing agent. The crystallite size calculated from XRD analysis using Scherrer's equation is found to be 2.32 and 3.13 nm for boehmite and γ-Al_2O_3 obtained by ultrasound stimulation, respectively, which is due to the formation of microjets during sonication. The particle size analysis result reveals the formation of nanosized γ-Al_2O_3 particles by ultrasonication with a mean particle size of 51 nm. In conclusion, the boehmite and γ-Al_2O_3 prepared by ultrasound stimulation are better than the samples synthesized by the conventional method.

1. Introduction

Owing to its unique properties such as high surface area, porosity, and chemical activity, γ-Al_2O_3 can be used in various applications including catalysts,[1] catalyst support,[2] adsorbents,[3] and membranes.[4] Boehmite (γ-AlOOH) is an important inorganic precursor in the production of γ-Al_2O_3. When it is heated, boehmite undergoes a topotactic transformation into γ-Al_2O_3 with a well-defined pore structure at around 600 °C.[5] Inherent relationships between the crystallinity of boehmite and material properties have been well studied in the past. Usually, crystalline boehmite provides γ-Al_2O_3 with lower surface area, and pseudoboehmite, consisting of low crystallinity, yields γ-Al_2O_3 with high surface area.[6,7] However, recent crystallographic studies indicated that pseudoboehmite is not strictly amorphous and consists of either a micro- or nanocrystalline structure.[8,9]

To date, two conventional routes exist for the synthesis of boehmite with controlled chemistry, morphology, and textural properties.[10] These are (a) hydrolysis of aluminum alkoxides and (b) precipitation from inorganic salts in an aqueous medium. Boehmite preparation using aluminum alkoxides is conducted at higher temperatures (above 80 °C) to yield a stable crystalline product. One of the major limitations of this route is that the operating temperatures have a predominant effect on the pore size and the surface area. While hot water hydrolysis of aluminum alkoxides at 90 °C yields stable crystalline boehmite, cold water hydrolysis produces bayerite at room temperature.[11,12] Major drawbacks in the hydrolysis synthesis route are high cost of alkoxides and their moisture sensitive-nature.[13] So there is always a genuine demand to develop metal oxides using cheap and easily available inorganic precursors. On the other hand, the route adopting the precipitation of inorganic salts in an aqueous medium appears to be more advantageous due to its ability to alter process variables to control the textural properties of γ-Al_2O_3. The precipitation route involves the addition of a base like NaOH or NH_4OH in aqueous medium to aluminum salts such as $AlCl_3$ and Al $(NO_3)_3$.[14] Some of the parameters in the precipitation route that influence the product textural properties include salt type,[15] mixing procedure,[16] pH value,[17] aging condition,[18] and the structure-directing agent.[19] Henceforth, the parametric study of the precipitation process assumes paramount significance as the parameters chosen can yield either bayerite or boehmite or gibbsite.[20] Recently, Mahmoodi et al.[21] demonstrated a quick, simple route to synthesize boehmite nanofibers by a direct reaction between activated aluminum and hot water. They obtained an average crystallite size of boehmite of about 4.3 nm. Gabelkov et al.[22] examined the evolution of the phase composition during the thermal decomposition of nanosized aluminum hydroxides precipitated from aluminum nitrate solution by direct and inverse precipitation. They reported that the nanosized γ-Al_2O_3 starts forming even at 570 K. In the work of He et al.,[23] a facile hydrothermal method has been used to synthesize boehmite nanorods with a length of 50−2000 nm and a diameter of 6−20 nm by treating the $Al(OH)_3$ gel in acidified sulfate solution at elevated temperatures. Later, they also investigated the coeffects of pH and the anions such as nitrate, chloride and sulfate on the morphology of boehmite.[24] They reported that under alkaline conditions (initial pH 10.5), boehmite nanoplates were produced irrespective of the anion types whereas under acidic conditions (initial pH 4.0), boehmite nanorods were formed in the presence of nitrate and chloride.[24]

* To whom correspondence should be addressed. Tel.: 91-361-2582264. Fax: 91-361-2582291. E-mail: pugal@iitg.ernet.in.
[†] Indian Institute of Technology Guwahati.
[‡] Indian Institute of Technology Delhi.

10.1021/ie901857q
Published on Web 04/23/2010

During precipitation/aging process of boehmite, precipitates will agglomerate because of its high surface energy. Different methods exist for breaking the agglomerates to yield a stable sol of boehmite, and hence materials with good textural characteristics can be obtained. Acid addition (peptization) at higher temperature is one of the conventional routes for deagglomeration and is a potentially slower process.[12] Even though peptization is relatively easier, it involves higher residence times (24−48 h) coupled with high agitation and reflux conditions. The conventional routes for dispersing particles into liquids, however, usually is not sufficient, since the nanoparticles tend to form very strong agglomerates requiring extremely high specific energy inputs in order to overcome the adhesive forces. Therefore ultrasound is one means to deagglomerate nanoparticles in aqueous dispersions.[25−28]

The origin of sonochemical effects in liquids is due to the phenomenon of acoustic cavitation.[29] Microjets and/or shock waves generated in the vicinity of the collapsing cavitational bubbles have been used for the size reduction of the material to the nanoscale. In the ultrasonic process, an acoustic cavitation process can generate a transient localized hot zone with extremely high temperature gradient and pressure. These high temperatures and pressures result in the generation of radicals due to dissociation of entrapped vapor molecules in the bubble.[30−32] These physical and chemical effects assist the destruction of the sonochemical precursor and the formation of nanoparticles.[33−40]

In the past several years, ultrasound treatment has widely been used in the preparation of many inorganic metal oxide nanomaterials such as CoO, TiO_2, SiO_2, ZrO_2, MnO_x, ZnO, mesoporous Al_2O_3, and others.[40−50] All of these materials exhibited evenly distributed size, good dispersion, and good performance. Recently, Chave et al.[46] studied the effect of sonication of the mesoporous alumina with ultrasound in aqueous solution in the pH range of 4−11 and temperature of 36−38 °C. They found that the textural properties of the solid product depend on the sonication time and pH of the solution. In another work reported by Thiruchitrambalam et al.,[51] an ultrasonic bath was used to prepare the stable sol of boehmite synthesized from aluminum metal. Bodisova et al.[52] reported that during gelation, orientation of boehmite crystallites can be altered by ultrasonication. Domingos et al.[53] also studied the structural changes of the γ-alumina induced by ultrasound during the aging of the boehmite. The mean pore size practically does not change while the mean crystallite size is about 25% greater in the sonicated sample over nonsonicated sample. For several applications, ultrasound has been proved suitable for dispersing particles homogeneously in a liquid.[39] Hence, our attention is drawn to the possibility of utilizing ultrasound as a tool to obtain a reduced particle size of boehmite (by deagglomerating the particles) and γ-Al_2O_3 having narrower particle size distribution with bigger pore size and larger pore volume.

The objective of this work is to prepare γ-Al_2O_3 with superior material characteristics through the coupling of ultrasound stimulation to the precipitation route, deploying cheaper raw materials such as $AlCl_3$. The characterization techniques involving TGA, XRD, FTIR, nitrogen adsorption−desorption, and particle size analysis have been deployed to identify optimal process conditions for the synthesis of nanosize γ-Al_2O_3 with superior textural properties.

2. Materials and Methods

2.1. Synthesis of γ-Al_2O_3. To study the influence of ultrasound and synthesis procedure on the properties of nanosized γ-Al_2O_3, we have prepared the boehmite sols using the following procedure. Aluminum chloride hexahydrate ($AlCl_3 \cdot 6H_2O$, 99.5%) (Merck, India), ammonium hydroxide solution (NH_4OH, 30 wt %) (Merck, India), and Millipore water was used as starting material. First, 4 wt % aluminum chloride solution was made using Millipore water at room temperature, and the insoluble impurities were filtered out using filter paper. The pH of the resulting solution was 3.5 as measured by digital pH meter (Consort C 863, Belgium). After that a precipitating agent, aqueous ammonia was added slowly into the above solution under vigorous stirring until the pH of the sol reached 9.0. Then the sol was divided into three parts (200 mL each having 1.815 wt % boehmite concentration). The first part of the sol was taken in a beaker and sonicated by employing a direct immersion of titanium horn for 2 h. A schematic diagram of the experimental setup used in the present study was shown in Figure 1. For sonication, a microprocessor based and programmable ultrasound processor was used (Sonics and Materials, model VCX 500). This processor had a frequency of 20 kHz with maximum power output of 500 W. The processor had variable power output control, which was set at 20% during experiments, resulting in consumption of 100 W power during sonication. In addition, the processor had the facilities of automatic frequency tuning and amplitude compensation, which ensure constant power delivery to ultrasound probe irrespective of the changes occurring in the liquid medium. During the ultrasonic treatment, a thermocouple was inserted into the sol in order to measure the temperature of the sol and the reaction cell was cooled by water at ambient temperature (25 °C). After ultrasonic treatment, homogeneous and lightly opalescent boehmite sol was obtained. Then it was filtered and washed with Millipore water several times until chloride ions were not detected by $AgNO_3$ solution. Finally it was dried in an oven at 80 °C for 24 h. The obtained sample hereafter was referred to as as-dried sample (S-D).

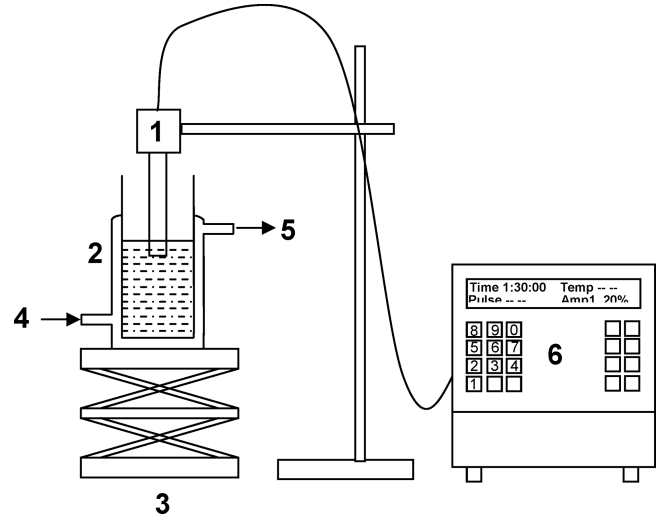

Figure 1. Schematic representation of ultrasonic horn sonication setup (1, ultrasound horn; 2, jacketed glass reactor; 3, laboratory jack; 4, cooling water inlet; 5, cooling water outlet; 6, control unit of ultrasonic processor).

For the second procedure (conventional heating method), another 200 mL of sol was transferred into a round-bottom flask with a reflux condenser and digested at 85 °C for 2 h (without ultrasound). After that, the sol was filtered, washed, and finally dried by following the same procedure mentioned above. In the third procedure, another 200 mL sol was aged at room temperature (25 °C) for 2 h (without ultrasound).

Then it was washed and dried as mentioned in the first procedure. Finally, all the three types of as-dried samples were calcined in a flow of air at 600 °C with a heating rate of 5 °C/min for 5 h to obtain γ-Al_2O_3. Thereafter, the samples were cooled to room temperature and used for analysis. The as-dried samples (boehmite) prepared by ultrasound stimulation, 85 °C (conventional heating method), and room temperature aging (25 °C) were denoted as S-D, 85-D, and 25-D, respectively. After calcining at 600 °C, the samples were denoted as S−C, 85-C, and 25-C, respectively.

2.2. Characterization. To identify phases and their crystallinity of the as-dried and calcined materials, X-ray powder diffraction (XRD) patterns were recorded in a Bruker AXS instrument using Ni filtered Cu Kα radiation (λ = 1.5406 Å) operating at 40 kV and 40 mA. Diffraction intensities were measured by scanning from 10 to 90° (2θ) with a step size of 0.05° per second. Weight loss and temperatures associated with phase transformations were determined by thermogravimetry (TG) and differential thermogravimetric (DTG) analysis. Thermogravimetric analyses of the samples were conducted in a TGA instrument of Mettler Toledo with model no. TGA 851^e in flowing air atmosphere at a heating rate of 10 °C min^{-1} from 25 to 900 °C to measure various decomposition reactions occurring in the as-dried precursor as a function of temperature. The transformation temperatures of boehmite to γ-Al_2O_3 were determined from the DTG curve.

The BET (Brunauer−Emmet−Teller) specific surface area, pore volume, and pore size distribution of the as-dried and calcined samples were determined by N_2 adsorption−desorption isotherms at 77 K measured in a surface area analyzer (Beckman-Coulter; model SA 3100). All the calcined samples were degassed at 250 °C for 12 h under vacuum (10^{-5} Torr) before recording their BET isotherms in a separate degassing unit attached to the instrument. The as-dried samples were degassed at a lower temperature of 100 °C in order to preserve its structure. The pore size distributions of the as-dried and calcined samples were verified by a BJH (Barrett−Joyner−Halenda) model from the adsorption branch of the nitrogen isotherms. The cumulative pore volume was calculated from the amount of nitrogen adsorbed up to a relative pressure, P/P_0 of 0.99 assuming all the pores are filled.

Dynamic light scattering equipment (HORIBA; model LB-550 V) with a He−Ne laser source was used to measure the size distributions of the particles. For all samples, the DLS measurements were performed at a scattering angle of 90°. The suspension was prepared by dispersing the powders in Millipore water at a constant temperature of 25 °C. The suspension was then treated to ultrasonic vibrations for a few minutes to declump the clusters.

3. Results and Discussions

Figure 2 shows the X-ray diffraction patterns of the as-dried samples (S-D, 85-D, and 25-D). The crystallographic structure of the materials after drying depends mainly on the hydrolysis condition. It can be seen from the figure that the as-dried precursor, 25-D (aged at room temperature) is amorphous, which is indicated by the broad peaks in the XRD pattern. The XRD patterns of S-D and 85-D samples match well with the boehmite phase, which is confirmed by the JCPDS file 21-1307. The absence of a doublet peak at 2θ = 18−21° also confirms that there is no bayerite phase in the material. The sample S-D, sonicated during digestion at room temperature, is composed of well-crystallized boehmite.

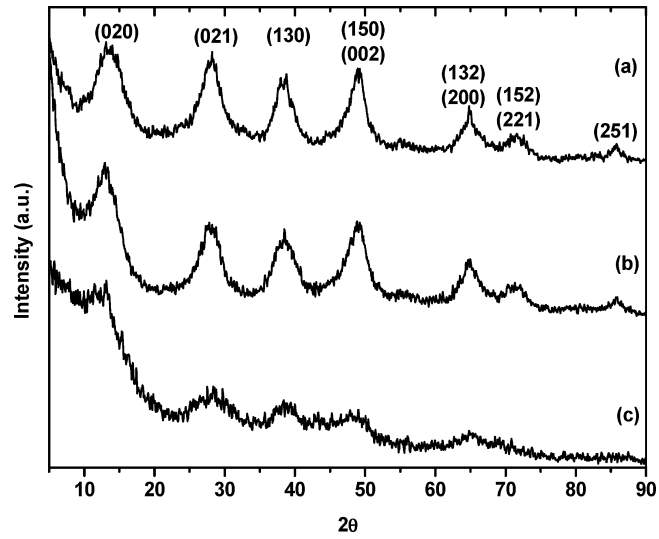

Figure 2. XRD pattern of (a) 85-D, (b) S-D, and (c) 25-D samples.

Formation of crystals at room temperature may be due to the birth of more numerous nuclei that leads to a greater surface area for growth. The 85-D sample, digested at 85 °C, maintains the same diffraction pattern of the boehmite phase like S-D sample. Figure 2 shows that the boehmite prepared by ultrasound (S-D) and digestion at 85 °C (85-D) appears to be more crystalline than that prepared at room temperature aging (25-D). It is documented in the literature that the intensities of the peaks vary significantly as a function of the synthesis conditions/methods.[54] For instance, such differences are especially true for the intensity ratios of the (021), (130), (150), and (002) peaks (see Figure 2a versus Figure 2b,c). More generally, the peak shape evolves with synthesis methods/conditions used. All these features are due to significant modifications of the size and shape of the boehmite particles.[54] The size of the boehmite crystallites is estimated from the broadening of the d (020)-peak using the Scherrer equation as presented in Table 1.

$$D_C = \frac{k\lambda}{\beta \cos \theta} \tag{1}$$

where k is a constant ~0.9, λ is the wavelength of the X-rays, β is the full width of diffraction peak at half-maximum intensity in radians, and θ is the Bragg angle.

The crystal size of the 25-D sample is not calculated due to broadening of the (020) peak. It is seen from Table 1 that the crystal size of the sonicated precursor is 2.32 nm, whereas the crystal size of the 85-D sample is 3.11 nm. The difference of crystal size can be explained by the sonication effect during aging. Two effects of sonication can be considered to explain the formation of nanosized crystal such as heat effects and mechanical effects. During the ultrasonic treatment, the temperature of the sol is maintained at constant temperature of 25 °C by cooling water circulation. So the heat effect is not the major parameter. The main event in sonochemistry is the creation, growth, and collapse of a bubble that is formed in the liquid. The stage leading to the growth of the bubble occurs through the diffusion of solute vapor into the volume of the bubble. Then the cavitation bubbles formed in the rarefaction cycle undergo unsymmetrical collapse near the solid surface, which causes "in-rush" of the liquid into the solid. This effect is called microjet formation or microstreaming, wherein the velocity of the in-rushing liquid is as high as

Table 1. Properties of As-Dried Precursors (Boehmite) and γ-Al_2O_3[a]

sample name	S_{BET} (m^2/g)	V_p (cm^3/g)	porosity (%)	D_p (nm)	d_{BET} (nm)	D_{DLS} (nm)	$D_{C(020)}$ (nm)	$D_{C(400)}$ (nm)	$d_{(020)}$ (nm)	transition temperature (°C)
S-D	351	0.287	46	3.23	5.7	38	2.32		0.683	373
85-D	325	0.243	42	3.00	6.1	58	3.11		0.673	391
25-D	201	0.143		2.85		283				362
S−C	256	0.388	59	6.06	6.4	51		3.13		
85-C	219	0.307	53	5.61	7.5	80		4.21		
25-C	191	0.245	47	5.13	8.6	936		3.93		

[a] S_{BET} = BET surface area; V_p = cumulative pore volume; D_p = pore diameter; d_{BET} = BET equivalent mean particle diameter; D_{DLS} = mean particle diameter obtained from DLS; D_C = crystalline size; d = spacing between the planes in the atomic lattice. S-D, S-C denotes the boehmite and γ-Al_2O_3, respectively, synthesized by ultrasound stimulation method. 85-D, 85-C denotes the boehmite and γ-Al_2O_3, respectively, synthesized by conventional heating method at 85°C. 25-D, 25-C denotes the boehmite and γ-Al_2O_3, respectively, synthesized at room temperature aging (25°C).

100 m/s.[55,56] Therefore, according to eq 2, the ultrasonic treatment can provide 55.55 kJ/mol energy, which is in agreement with the bond energy of weak bonds such as the hydrogen bond or van der Waals force.

$$w = \frac{1}{2}\frac{m}{M}v^2 = \frac{1}{2}\frac{V\rho}{M}v^2 = 55.55 \text{ kJ/mol} \qquad (2)$$

where the density of the bulk liquid medium $\rho = 1000$ kg/m^3; the volume of liquid medium $V = 200$ mL; the molar mass of water $M = 18$ g/mol; and the velocity $v = 100$ m/s.

The reason for getting nanostructured products is that the fast kinetics does not permit the growth of the nuclei, and in each collapsing bubble, a few nucleation centers are formed whose growth is limited by the short collapse. The ultrasonic treatment is able to provide enough energy to break down weak bonds which lead to particle aggregation. Thus sonication can produce homogeneous sol at room temperature. At higher digestion temperature, crystal size is more due to the thermally activated crystal growth and may be due to the fast ripening process at 85 °C that assists the generation of the crystalline boehmite.

The (020) peak of the boehmite (S-D) synthesized by ultrasound stimulation has been shifted to a higher d value (0.683 nm) as compared to the 85-D sample (0.673 nm). These values are in accordance with the crystal size as presented in Table 1. Two reasons have been proposed for this expansion of the d-spacing: such as excess interlayer water, x ($AlOOH \cdot xH_2O$), and effect of sonication. From the DTG analysis (see Figure 5), we did not get any peak indicating the loss of interlayer water for the S-D sample, so the other possible reason for the increase in d-spacing may be mentioned here. As discussed earlier, during sonication, cavitation occurs resulting in microjet formation. This may be the cause of higher value of d-spacing of the sonicated sample. Recently, a few researchers have demonstrated that the (020) peak shift is essentially due to a particle-size effect like the one observed for clays.[57−60] Figure 3 shows the XRD patterns of γ-Al_2O_3 powder obtained by calcination of as-dried boehmite precursor precipitated at various conditions under constant pH and digestion time. Figure 3a indicates that the formation of poorly crystallized alumina and broad peaks indexed for γ-Al_2O_3 are seen in the XRD patterns. However, all the peaks shown in Figure 3b,c are indexed for γ-Al_2O_3 having structure of an fcc sublattice of oxygen atoms. The crystallite size of γ-Al_2O_3 calculated using d (400) peak is reported in Table 1. The broadening of the diffraction pattern of sonicated sample reveals the formation of nanosized γ-Al_2O_3.

The thermogravimetric (TG) curves for as-dried precursors are depicted in Figure 4. The as-dried precursors appear to undergo two stages of decomposition for S-D and 25-D samples,

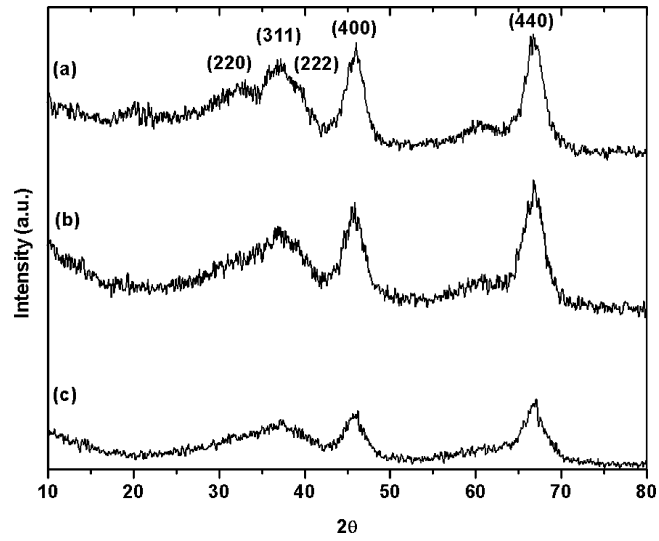

Figure 3. XRD pattern of (a) 85-C, (b) S-C, and (c) 25-C samples.

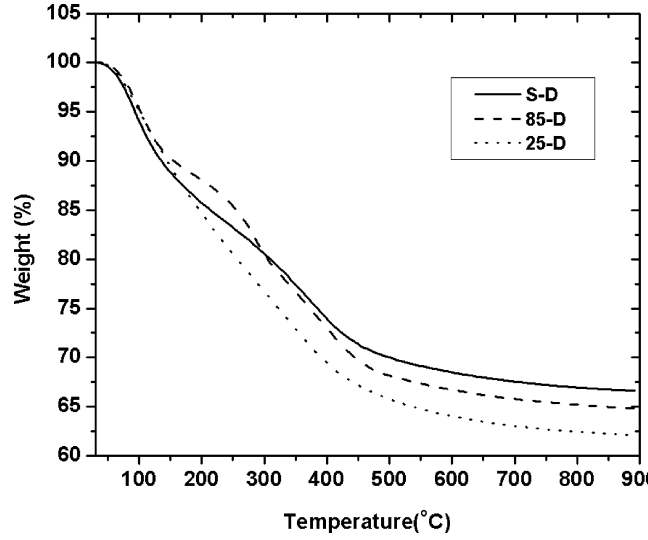

Figure 4. TGA of the as-dried samples.

whereas for 85-D sample one additional stage of decomposition takes place. The evolution of the weight loss with temperature is classical for this type of material. The first stage of decomposition (<110 °C) is the liberation of physically adhered water present in the pores. The final step (>362 °C) corresponds to dehydroxylation of boehmite to γ-Al_2O_3.[61] The additional second step (110−350 °C) for the 85-D sample can be assigned to the removal of the crystal water in the sample. The differential thermogravimetric (DTG) analysis of the as-dried precursors is presented in Figure 5. The first endothermic peak around 100 °C corresponds to the removal of water molecules adsorbed on

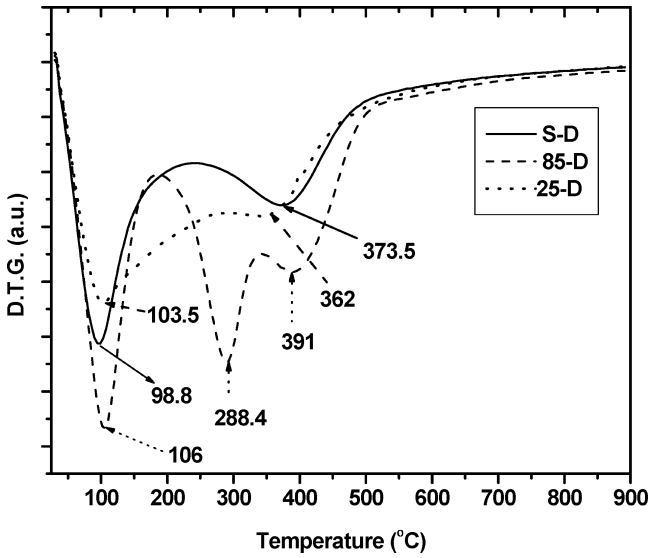

Figure 5. DTG of the as-dried samples.

the gel. The second endothermic peak around 360−390 °C is ascribed to boehmite decomposition to produce γ-Al_2O_3, involving elimination of OH groups, which is started by the following reaction:[61]

$$2AlOOH \rightarrow Al_2O_3 + H_2O \quad (3)$$

The DTG curve for 85-D sample shows an additional endothermic peak at about 288 °C that corresponds to the loss of crystal water from this sample. If the single phase boehmite is precipitated, then the total weight loss of ~15% would have been expected by reaction 3 leading to the formation of γ-Al_2O_3 powder. From the TGA analysis, the total weight loss is found to be 33, 35, and 38% for S-D, 85-D, and 25-D samples, respectively. These additional losses in TGA curves may be related to adsorption of water in boehmite. As presented in Table 1, for a corresponding increase in the crystallite size (D_c) of boehmite, the transition temperature of boehmite to γ-Al_2O_3 (and hence thermal stability) also increases.

According to the kinetic study of γ-Al_2O_3 formation by Tsuchida et al.,[62] the mechanism depends on the crystallite size of boehmite, being nucleation controlled in large crystallites, phase-boundary controlled in medium-sized crystallites, and diffusion controlled in small crystallites. The conversion from boehmite to γ-Al_2O_3 includes dehydration. The crystal structure of boehmite consists of Al−O octahedral double layers, which are connected by hydrogen bonds.[63] The dehydration path inside the boehmite structure is therefore believed to be along the *ac* plane. In smaller crystallites of boehmite, this path becomes shorter, and the interlayer spacing is broad. Dehydration occurs rapidly and enhances the conversion of boehmite to γ-Al_2O_3 and decreases the formation temperature of γ-Al_2O_3.[64] So the modification of transition temperature for the sonicated sample is due to the smaller particle size formed by sonication treatment. From the TG and DTG graphs, one can get the preliminary idea about the effect of sonication in terms of crystallite size in correspondence with transition temperature.

Surface area and pore volume of the as-dried and calcined samples aged at different conditions at constant pH are given in Table 1. The surface area (S_{BET}) of the boehmite obtained by sonication (S-D) is higher than the conventional heating method (85-D) and room temperature aging sample (25-D). The variation of surface area may be related to the agglomerated structure of boehmite particles since the high S_{BET} of boehmite arises from spaces formed by agglomeration of fine boehmite particles of suitable size. There is an optimum particle size to produce a high S_{BET} in boehmite. Upon controlled calcination at 600 °C, the surface area of the samples is decreased with an increase in the pore volume and pore diameter. This may be due to the removal of structural water during the transformation to the oxide.

Porosity (eq 4) and average pore diameter (eq 5) are calculated based on surface area, cumulative pore volume (V_{pore}), and density of the boehmite and γ-Al_2O_3 (ρ_p)

$$\text{porosity (\%)} = 100\left(\frac{\rho_P V_{pore}}{1 + \rho_P V_{pore}}\right) \quad (4)$$

$$\text{average pore diameter } (D_p) = \frac{4V_{pore}}{\text{surface area}} \quad (5)$$

Assuming the density value reported in the literature (3.01 g/cm^3 for crystalline boehmite and 3.65 g/cm^3 for γ-Al_2O_3), the estimated porosity of the boehmite and γ-Al_2O_3 is presented in Table 1. The porosity and average pore diameter are maximum for as-dried sonicated precursor (S-D) and minimum for 25-D sample. The average pore diameter of the γ-Al_2O_3 is found to increase upon calcination depending on the pore diameter of the as-dried precursor. The enhancement in porosity for S-D sample is due to the sonication effect during aging. The presence of amorphous material in the 25-D sample can be expected to reduce the surface area and the pore volume of the resultant γ-Al_2O_3 since the amorphous solid would act as a pore filler. A higher value of surface area, cumulative pore volume, and pore diameter is obtained for the S-D (and S-C) sample when compared with the 85-D (and 85-C) sample and those reported by Chuah et al.[18] They have synthesized aluminum hydroxide with a pore volume of 0.20 mL g^{-1} and surface area of 59.3 m^2 g^{-1} after 24 h aging.[18] In this work, we have synthesized boehmite with better textural properties with 2 h aging. γ-Al_2O_3 obtained in our case has a higher surface area (256 m^2 g^{-1}), larger cumulative pore volume (0.388 cm^3 g^{-1}), and bigger pore diameter (6.06 nm) when compared to γ-Al_2O_3 synthesized by Chuah et al.[18] They obtained the γ-Al_2O_3 with surface area, pore volume, and pore diameter of 239 m^2 g^{-1}, 0.26 cm^3 g^{-1}, and 4.27 nm, respectively for the sample aged at room temperature for 24 h. Moreover, the γ-Al_2O_3 synthesized by ultrasound stimulation is better than one of the commercial γ-Al_2O_3 (Alcoa H-156) used in petroleum refinery industries (manufactured by Alcoa World Chemicals, Houston, TX).[65] The surface area, pore volume, and average pore diameter of this material is reported as 177 m^2 g^{-1}, 0.238 cm^3 g^{-1}, and 5.4 nm, respectively.[65]

N_2 adsorption−desorption isotherms of all the as-dried and calcined samples are shown in Figures 6 and 7, respectively. All the calcined samples show a reversible part in the isotherm in a low relative pressure range and a hysteresis loop in a higher pressure range. The amount of nitrogen adsorbed at higher relative pressure (P/P_0) differs greatly from sample to sample depending upon the aging condition. The increase in the total adsorption is reflected in the total pore volume value. Analysis of the hysteresis loop is done based on the classification given by DeBoer.[66] The entire as-dried precursor (except 25-D) shows type E, which is characterized by a sloping adsorption branch and a steep desorption branch at intermediate relative pressure. This type of hysteresis loop may appear in tubular or ink-bottle pores with bodies of varying widths. Generally, the formation of pores is spaces between the particles and so the shape of the

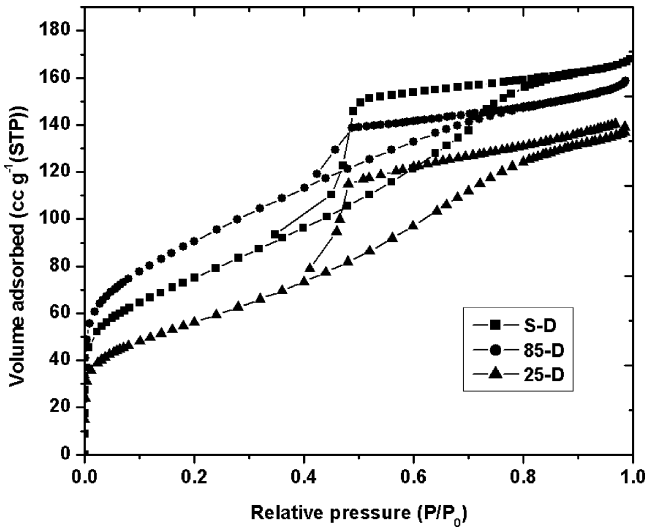

Figure 6. Nitrogen adsorption/desorption isotherms of the as-dried samples.

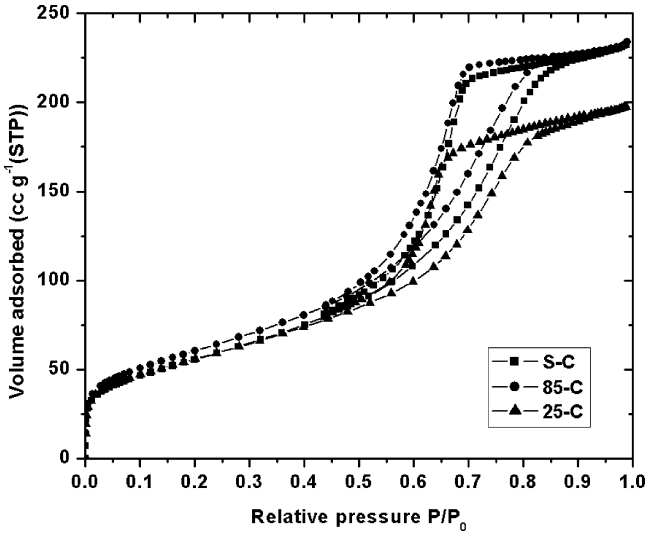

Figure 7. Nitrogen adsorption/desorption isotherms of calcined sample.

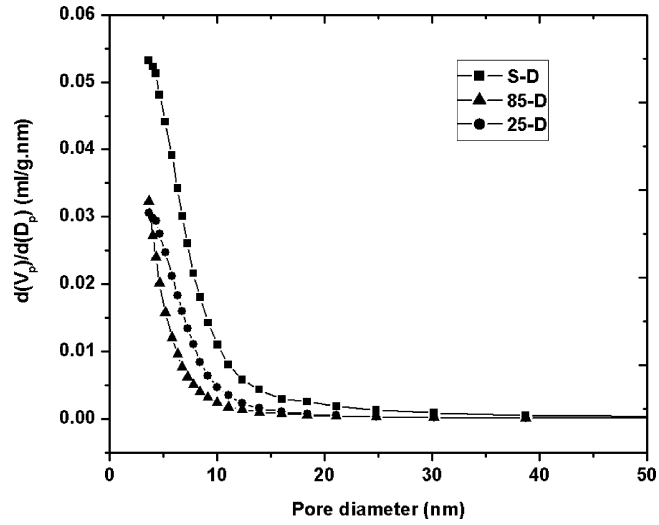

Figure 8. BJH pore size distribution of the as-dried samples.

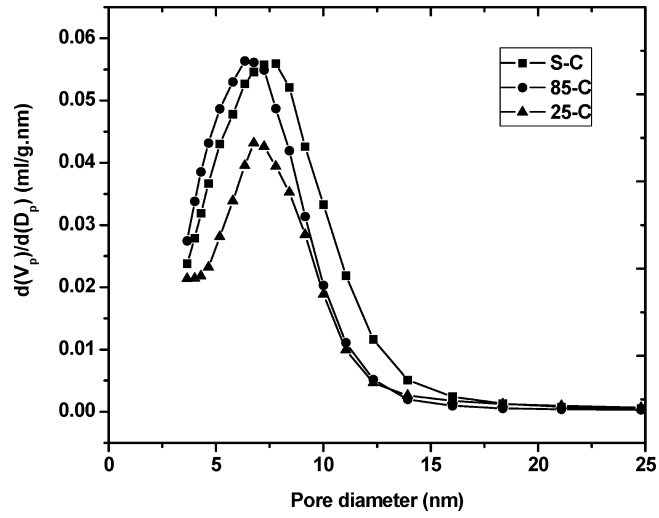

Figure 9. BJH pore size distribution of calcined samples.

pores is influenced by the shape of the particles. If there are slit-shaped pores between such plate-like particles, capillary condensation does not occur until the pressure of nitrogen is saturated, as pores with open ends on both sides cannot form menisci. However, they did show capillary condensation at intermediate relative pressure. Therefore, this led to the conclusion that the pores in this system are formed between cubic particles, which are built in layers with the plate-like particles. The hysteresis loop of type B is observed for the 25-D sample as defined by slit-shaped pores. All the calcined samples show the hysterisis loop of type E.

Generally, the desorption branch is selected for the calculation of pore size distribution. But a recent study suggests that the calculation of pore size distribution of the samples having an E-type hysteresis loop has to be done using the adsorption branch and not the desorption branch.[67] This is due to the location of desorption that is largely controlled by network-percolation effects. So the pore size distribution is obtained according to the Barrett−Joyner−Halenda (BJH) method using adsorption data as shown in Figure 8 (as-dried sample) and Figure 9 (calcined sample). These plots confirm that the pore sizes of all the samples are in the mesoporous range. There is no pore size distribution observed below 3 nm because of the incapability of the BET surface area analyzer.[68] The pore size distribution of S-D sample has pores predominantly less than 5 nm. All the calcined samples have unimodal narrow pore size distributions with pores around 3.6−8 nm in diameter. However under ultrasound stimulation, the distribution shifts toward larger pore sizes. The micropore volume of all the samples calculated by the *t*-plot technique is found to be zero. So the mesoporous nanosized γ-Al_2O_3 with bigger pore diameter and larger cumulative pore volume can be prepared by using ultrasound stimulation during aging of boehmite. Generally, the mesoporous alumina was prepared by using organic templates to form and adjust pore size. The BET equivalent mean particle diameters, d_{BET}, is calculated using the following expression:

$$d_{BET} = \frac{6}{\rho_P S_{BET}} \tag{6}$$

In eq 6, ρ_p and S_{BET} stand for the bulk density of particle and the BET surface area. The calculated d_{BET} values are presented in Table 1.

To confirm the formation of nanosized particles, we have also carried out DLS measurements. Figure 10 illustrates the particle size distributions of the as-dried precursors (boehmite) and calcined samples (γ-Al_2O_3). The mean particle diameter obtained from DLS measurement is listed in Table 1. The decrease of

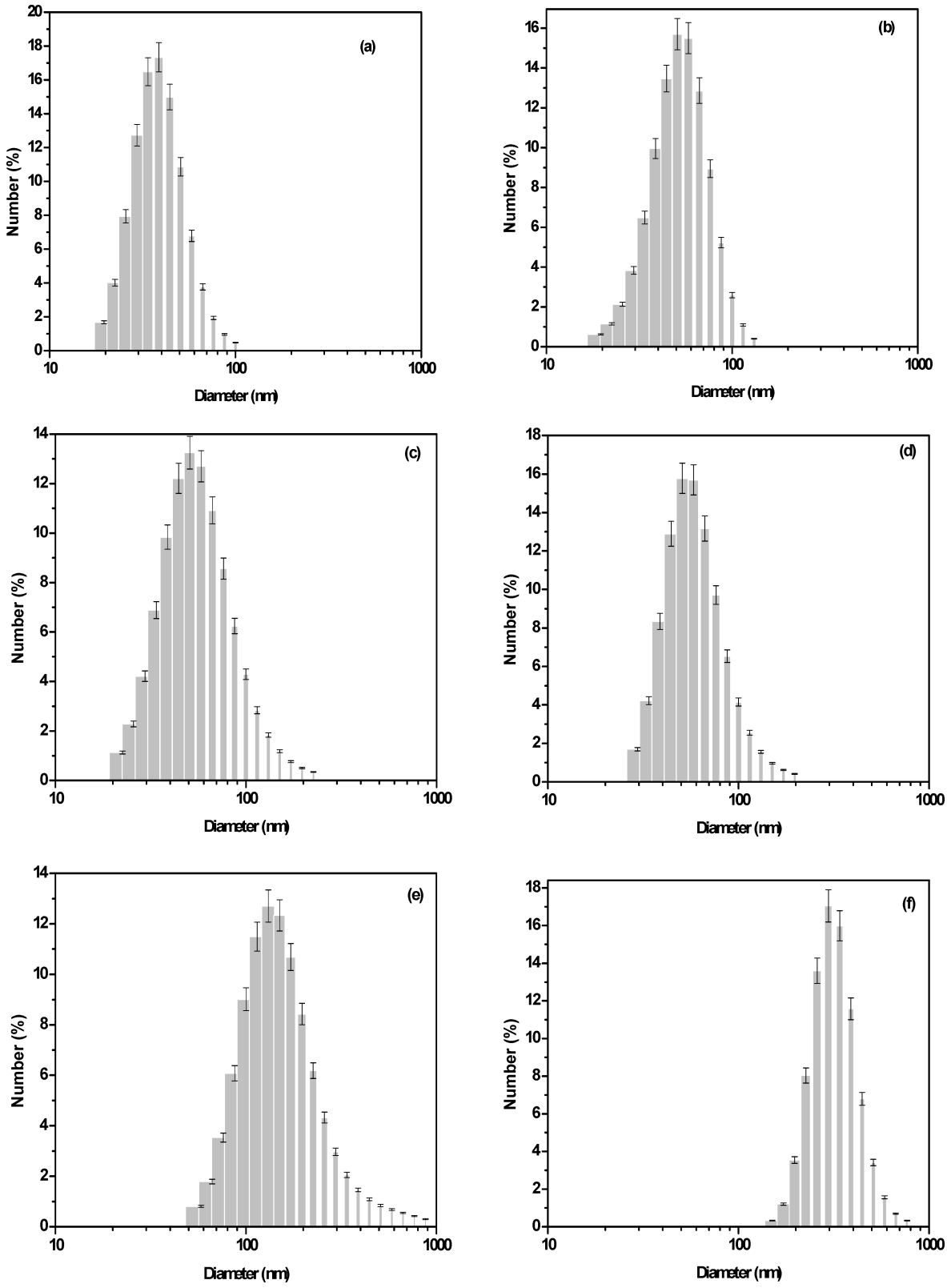

Figure 10. DLS particle size distribution of (a) S-D, (b) S-C, (c) 85-D, (d) 85-C, (e) 25-D, and (f) 25-C samples.

particle size by ultrasound stimulation for both the as-dried precursor and calcined sample is clearly visible. The discrepancy between the crystal size and mean particle size by DLS measurement is due to the agglomeration of particles. This is because we did not apply ultrasound more than 2 min before DLS measurement, as our primary objective was the study of the effect of ultrasound. There is a shift in particle size distribution toward the left for both the S-D and S-C samples as compared to the 85-D and 85-C samples as well as the 25-D and 25-C samples. The tendency of formation of agglomerates is higher for the 25-D sample as the mean particle size is well above 100 nm.

In many cases, it has been observed that by refluxing the same precursors used in the sonochemical process, identical nanoproducts to those obtained sonochemically can be obtained either solvothermally or even in an open heated reaction.[38]

However, ultrasound irradiation enables the generation of smaller particles having narrow particle size distribution with higher surface area, larger pore volume, and bigger pore size. The conventional heating/hydrothermal methods are generally more successful in producing weakly agglomerated powders but the crystalline size tends to be considerably larger as presented in Table 1. Therefore, the advantages of sonication versus the conventional method of preparing nanomaterials includes the more uniform distribution/dispersion of the nanoparticles, better surface area, pore size and pore volume, and lower average particle size.

Surface area, average particle size, and pore diameter of the nanomaterials are all contributing factors to the catalytic reaction. It can be seen from Table 1 that the nanosized γ-Al_2O_3 prepared by the ultrasound technique has a higher surface area, bigger pore diameter, larger cumulative pore volume, and lower average particle size. In the work of Neppolian et al.,[34] it was experimentally proven that the degradation of 4-chlorophenol was higher when smaller sized particles with larger pore diameters of TiO_2 was used as a catalyst. Awati et al.[39] reported that photocatalytic decomposition of methylene blue using nanocrystalline TiO_2 showed lower decomposition capacity for higher particle size of TiO_2.

To compare the performance of the ultrasound method with conventional heating (85 °C) for the synthesis of boehmite, we have estimated the energy, work index, and cost involved in the two synthesis routes based on the procedure reported elsewhere.[33] The energy dissipated per kg of the boehmite for each case has been calculated, and the detailed procedure of calculation is given in the Appendix I. For the ultrasonic method, actual power delivered was 6.97 W with the original boehmite volume being 20×10^{-5} m^3 (equivalent to 3.63×10^{-3} kg of boehmite) giving a net energy dissipation rate of 34.85×10^3 W/m^3. Based on the boehmite concentration (1.815%), the energy dissipated per kg of the boehmite size reduced has been calculated (J/kg). The energy dissipation per kg of the boehmite is estimated to be 13.82×10^6 and 4.96×10^8 J/kg for ultrasonic stimulation and conventional heating methods (85 °C), respectively. This indicates that the energy dissipation by ultrasound stimulation is over 1 order of magnitude less than the conventional method. The total energy utilized for increasing surface area, pore diameter, pore volume, and reducing the particle size of the boehmite is found to be 5.01×10^4 J for ultrasonic technique which is 2 orders of magnitude less than the conventional heating method (1.8×10^6 J). The energy required to create a new surface area is calculated to be 92 and 3999 N/m for the ultrasonic and conventional heating methods, respectively. It again confirms a reduction of 2 orders of magnitude for the ultrasonic method. For the same material processing, it is possible to find out the right technique for the size reduction from the knowledge of work index (WI) for various equipments. The WI values for the material (boehmite) processed, to reduce the particle size by ultrasound (from 283 to 38 nm) and conventional method (from 283 to 58 nm), are estimated to be 1271.54 and 12124, respectively. All the costs reported in this work are based on the operating cost (electricity consumption). The amount of electricity required for operating the equipment to obtain smaller particles of boehmite having good surface area, pore size, and pore volume was calculated using the initial and final average size of the particle. A sample calculation is given in Appendix I. The ultrasonication method appears significantly cost-effective in reducing the size of boehmite with higher surface area, bigger pore size, and larger pore volume. The operating costs for obtaining nanosized boehmite by the ultrasound stimulation and the conventional heating technique are found to be Rs. 193 and Rs. 964 per kg of boehmite, respectively. The cost and energy estimation reported in this work is performed only for the synthesis of boehmite using the two routes because the same equipment is used for converting boehmite to γ-Al_2O_3 by calcination at 600 °C.

4. Summary

γ-Al_2O_3 with a crystallite size of 3.13 nm has been successfully prepared by ultrasound stimulation during the aging of boehmite. The main effect of sonication is to produce sufficient energy to break the agglomerates during aging resulting in smaller crystallite size. The γ-Al_2O_3 obtained by ultrasound stimulation has higher surface area (256 m^2 g^{-1}), bigger pore diameter (6.06 nm), and larger cumulative pore volume (0.388 cm^3 g^{-1}) than the conventional heating method (surface area, pore diameter, and pore volume of 219 m^2 g^{-1}, 5.61 nm, 0.307 cm^3 g^{-1}, respectively), which are even higher than the value reported in the literature (pore diameter of 4.27 nm and pore volume of 0.26 cm^3 g^{-1}). The room temperature aged precursor shows noncrystallized boehmite, and the surface area of the resulting γ-Al_2O_3 is very low. The particle size analysis reveals the agglomerate sizes of the room temperature aged sample, whereas the particle size of the sonicated as-dried precursor as well as γ-Al_2O_3 is the lowest. Therefore it can be concluded that the ultrasound stimulation method may be an alternative route to the production of γ-Al_2O_3 with a higher surface area, bigger pore diameter, and larger pore volume without using any structure directing agent.

Acknowledgment

The authors are grateful to Centre for Nanotechnology of IIT Guwahati for help with XRD and DLS analysis and Department of Chemistry for FTIR analysis. We wish to express our sincere thanks to Dr. T. Sivasankar (Department of Chemical Engineering, NIT Trichy, India), Dr. V. S. Moholkar (Department of Chemical Engineering, IIT Guwahati), and Dr. M. Sivakumar (Department of Chemical & Environmental Engineering, University of Nottingham, Malaysia) for their helpful discussion in ultrasonication and Dr. R.G. Uppaluri (Department of Chemical Engineering, IIT Guwahati) for his helpful discussion in energy and cost estimation.

Appendix

Energy and Cost Estimations. The specifications of the ultrasonic horn are as follows: make, VCX 500; frequency, 20 kHz; rated output power used =100 W; calorimetric efficiency[69] = 6.97%; diameter of horn = 1.3×10^{-2} m; surface area of ultrasound irradiating face = 1.33×10^{-4} m^2.

To determine the calorimetric efficiency, a 200 mL volume of sample was irradiated with ultrasound (100 W power) for a known period of time (t), and the rise in temperature of the solution was measured. The following equation is used to calculate the actual rate of energy input to the system:

$$\frac{mc_p\Delta T}{t} = \frac{0.2 \times 4180 \times 5}{600}\frac{\text{Joule}}{\text{seconds}} = 6.97\ \text{W} \qquad \text{(A1)}$$

$$\text{calorimetric efficiency} = \frac{6.97\ \text{W}}{100\ \text{W}} \times 100 = 6.97\%$$

A 1.815% boehmite solution having initial particle size of 283 nm was irradiated by ultrasound for 120 min to result an average final particle size of 38 nm.

Net energy dissipated = 100 J/s × 120 min × 60 s/min × 0.0697 = 50184 J.

Energy dissipated per unit volume of liquid = (100 × 0.0697)/(20 × 10^{-5}) = 34.85 × 10^3 W/m^3.

Net energy dissipated per kg of boehmite = 50184/3.63 × 10^{-3} = 13.82 × 10^6 J/kg.

Total energy utilized for increasing surface area, pore size, pore volume, and reducing the particle size of the boehmite = 50184 J.

Increasing surface area after sonication = (351 − 201) m^2/g × 3.63 g = 544.5 m^2.

So, energy utilized to create new surface area = 50184/544.5 J/m^2 = 92.16 N/m.

Energy required for size reduction in terms of work index (W_i) calculation:

$$\frac{P}{m} = 0.3162 \times W_i \times \left(\frac{1}{\sqrt{D_{pb}}} - \frac{1}{\sqrt{D_{pa}}}\right) \qquad \text{(A2)}$$

where P is the power required in kW; m is the solid flow rate in tons/h; D_{pa}, D_{pb} is the initial and final size in mm (assumed spherical particle).

Solid flow rate = 2.42 × 10^{-3} kg/h = 2.42 × 10^{-6} tons/h.

Power supplied = 100 W = 0.1 kW.

D_{pa} = 283 × 10^{-6} mm, D_{pb} = 38 × 10^{-6} mm.

The work index to reduce the particle size from 283 to 38 nm by ultrasound is estimated to be 1271.54.

Electrical power consumed = 100 W × 2 h = 0.2 kWh.

Cost of the electricity = 0.2 kWh × 3.5 Rs./kWh = Rs. 0.7.

Total electrical cost = 0.7 Rs./(3.63 × 10^{-3}) kg of boehmite = 193 Rs./kg.

So the operating cost for getting 38 nm sized boehmite having surface area of 351 m^2/g, pore size of 3.27 nm and pore volume of 0.287 cm^3/g is Rs. 193 per kg.

Technique 2: Conventional Heating. The power of the heater used = 500 W; the efficiency of heater = 50% (assumed).

Net energy dissipated = 1.8 × 10^6 J.

Energy dissipated per unit volume of liquid = 1.25 × 10^6 W/m^3.

Net energy dissipated per kg of boehmite = 4.96 × 10^8 J/kg.

Total energy utilized for increasing surface area, pore size, pore volume and reducing the particle size of the boehmite = 1.8 × 10^6 J.

So, energy utilized to create new surface area = 3999 N/m.

The work index to reduce the particle size from 283 to 58 nm by conventional heating is estimated to be 12124.

Electrical power consumed = 500 W × 2 h = 1 kWh.

Cost of the electricity = 1 kWh × 3.5 Rs./kWh = Rs. 3.5.

Total electrical cost = 3.5 Rs./(3.63 × 10^{-3}) kg of boehmite = 964 Rs./kg.

So the operating cost for getting 58-nm sized boehmite having a pore size of 3.0 nm and pore volume of 0.243 cm^3/g is Rs. 964 per kg.

Literature Cited

(1) Ching, W. Y.; Xu, Y. N. First-Principles Calculations of Electronic, Optical, and Structural Properties of α-Al_2O_3. *J. Am. Ceram. Soc.* **1994**, *77*, 404.

(2) Li, G.; Smith, R. L., Jr.; Inomata, H.; Arai, K. Synthesis and Thermal Decomposition of Nitrate-Free Boehmite Nanocrystals by Supercritical Hydrothermal Conditions. *Mater. Lett.* **2002**, *53*, 175.

(3) Priya, G. K.; Padmaja, P.; Warrier, K. G. K.; Damodaran, A. D.; Aruldhas, G. Dehydroxylation and High Temperature Phase Formation in Sol−Gel Boehmite Characterized by Fourier Transform Infrared Spectroscopy. *J. Mater. Sci. Lett.* **1997**, *16*, 1584.

(4) El-Katatny, E. A.; Halawy, S. A.; Mohamed, M. A.; Zaki, M. I. A Novel Synthesis of High-Area Alumina via H_2O_2-Precipitated Boehmite from Sodium Aluminate Solutions. *J. Chem. Technol. Biotechnol.* **1998**, *72*, 320.

(5) Raybaud, P.; Digne, M.; Iftimie, R.; Wellens, W.; Euzen, P.; Toulhoat, H. Morphology and Surface Properties of Boehmite (γ-alooh): A Density Functional Theory Study. *J. Catal.* **2001**, *201*, 236.

(6) Wefers, K.; Bell, G. M. Oxide and Hydroxide of Aluminum . *Alcoa Technical Paper No.19*; Alcoa Laboratories: Pittsburgh, PA, 1987.

(7) Bagwell, R. B.; Messing, G. L. Critical Factors in the Production of Sol−Gel Derived Porous Alumina. *Key Eng. Mater.* **1996**, *115*, 45.

(8) Bokhimi, X.; Toledo-Antonio, J. A.; Guzman-Castillo, M. L.; Hernandez-Beltran, F. Relationship between Crystallite Size and Bond Lengths in Boehmite. *J. Solid State Chem.* **2001**, *159*, 32.

(9) Gobichon, A. E.; Rebours, B.; Euzen, P. Thermal Study of a Precursor for Catalyst Supports: Well- and Microcrystallised Boehmites. *Mater. Sci. Forum.* **2001**, *523*, 378.

(10) Music, S.; Dragcevic, D.; Popovic, S. Hydrothermal Crystallization of Boehmite from Freshly Precipitated Aluminum Hydroxide. *Mater. Lett.* **1999**, *40*, 269.

(11) Yoldas, B. E. Alumina Gels That Form Porous Transparent Al_2O_3. *J. Mater. Sci.* **1975**, *10*, 1856.

(12) B, E. Yoldas, Alumina Sol Preparation from Alkoxides. *Am. Ceram. Soc. Bull.* **1975**, *54*, 289.

(13) Brinker, C. J.; Scherrer, G. W. *Sol-Gel Science: The Physics and Chemistry of Sol-Gel Processing*; Academic Press: Boston, 1990.

(14) Trimm, D. L.; Stanislaus, A. Control of Pore Size in Alumina Catalyst Supports: A Review. *Appl. Catal.* **1986**, *21*, 215.

(15) Mishra, D.; Anand, S.; Panda, R. K.; Das, R. P. Effect of Anions during Hydrothermal Preparation of Boehmites. *Mater. Lett.* **2002**, *53*, 133.

(16) Hochepieda, J. F.; Ilioukhinaa, O.; Berger, M. H. Effect of the Mixing Procedure on Aluminium (Oxide)-Hydroxide Obtained by Precipitation of Aluminium Nitrate with Soda. *Mater. Lett.* **2003**, *57*, 2817.

(17) Okada, K.; Nagashima, T.; Kameshima, Y.; Yasumori, A.; Tsukada, T. Relationship between Formation Conditions, Properties, and Crystallite Size of Boehmite. *J. Colloid Interface Sci.* **2002**, *253*, 308.

(18) Chuah, G. K.; Jaenicke, S.; Xu, T. H. The Effect of Digestion on the Surface Area and Porosity of Alumina. *Microporous Mesoporous Mater.* **2000**, *37*, 345.

(19) Liu, Q.; Wang, A.; Wang, X.; Zhang, T. Mesoporous γ-Alumina Synthesized by Hydrocarboxylic Acid as Structure-Directing Agent. *Microporous Mesoporous Mater.* **2006**, *92*, 10.

(20) Lippens, B. C.; Steggerda, J. J. In *B.G. Physical and Chemical Aspects of Adsorbents and Catalysts*; Academic Press: London, 1970.

(21) Mahmoodi, K.; Alinejad, B. Fast and Facile Synthesis of Boehmite Nanofibers. *Powder Technol.* **2010**, *199*, 289.

(22) Gabelkov, S. V.; Tarasov, R. V.; Poltavtsev, N. S.; Kurilo, Y. P. Evolution of Phase Composition in the Thermal Decomposition of Nanosized Aluminium Hydroxides. *Powder Metallur. Metal Ceram.* **2009**, *48*, 478.

(23) He, T.; Xiang, L.; Zhu, S. Hydrothermal Preparation of Boehmite Nanorods by Selective Adsorption of Sulfate. *Langmuir* **2008**, *24*, 8284.

(24) He, T.; Xiang, L.; Zhu, S. Different Nanostructures of Boehmite Fabricated by Hydrothermal Process: Effects of pH and Anions. *Cryst. Eng. Commun.* **2009**, *11*, 1338.

(25) Guo, Q.; Zheng, S.; Tao, W.; Su, D. Experimental Research on the Ultrasonic Nanometer Grinder. *Mater. Lett.* **2007**, *61*, 3106.

(26) Markovic, S.; Mitric, M.; Starcevic, G.; Uskokovic, D. Ultrasonic De-Agglomeration of Barium Titanate Powder. *Ultrason. Sonochem.* **2008**, *15*, 16.

(27) Nyborg, W. L. M. *Acoustic Streaming*; Academic Press: New York, 1965.

(28) Noltingk, B. E.; Neppiras, E. A. Cavitation Produced by Ultrasonics. *Proc. Phys. Soc.* **1950**, *63B*, 674.

(29) Abramov, O. *Ultrasound in Liquid and Solid Metals*; CRC Press: Boca Raton, FL, 1994.

(30) Sutkar, V. S.; Gogate, P. R. Design Aspects of Sonochemical Reactors: Techniques for Understanding Cavitational Activity Distribution and Effect of Operating Parameters. *Chem. Eng. J.* **2009**, *155*, 26.

(31) Sutkar, V. S.; Gogate, P. R.; Csoka, L. Theoretical Prediction of Cavitational Activity Distribution in Sonochemical Reactors. *Chem. Eng. J.* **2010**, *158*, 290.

(32) Sutkar, V. S.; Gogate, P. R. Mapping of Cavitational Activity in High Frequency Sonochemical Reactor. *Chem. Eng. J.* **2010**, *158*, 296.

(33) Patil, M. N.; Pandit, A. B. Cavitation−A Novel Technique for Making Stable Nanosuspensions. *Ultrason. Sonochem.* **2007**, *14*, 519.

(34) Neppolian, B.; Wang, Q.; Jung, H.; Choi, H. Ultrasonic-Assisted Sol-Gel Method of Preparation of TiO_2 Nanoparticles: Characterization, Properties and 4-Chlorophenol Removal Application. *Ultrason. Sonochem.* **2008**, *15*, 649.

(35) Yao, N.; Xiong, G.; Sheng, S.; He, M.; Yang, W.; Bao, X. Ultrasound as a Tool to Synthesize Nano-Sized Silica-Alumina Catalysts with Controlled Mesoporous Distribution by a Novel Sol-Gel Process. *Catal. Lett.* **2002**, *78*, 37.

(36) Kim, K. H.; Kim, K. B. Ultrasound Assisted Synthesis of Nano-Sized Lithium Cobalt Oxide. *Ultrason. Sonochem.* **2008**, *15*, 1019.

(37) Sauter, C.; Emin, M. A.; Schuchmann, H. P.; Tavman, S. Influence of Hydrostatic Pressure and Sound Amplitude on the Ultrasound Induced Dispersion and De-Agglomeration of Nanoparticles. *Ultrason. Sonochem.* **2008**, *15*, 517.

(38) Sivakumar, M.; Gedanken, A.; Zhong, Z.; Chen, L. Acoustic Cavitaion-An Efficient Energetic Tool to Synthesize Nanosized $CuO-ZrO_2$ Catalysts with a Mesoporous Distribution. *New J. Chem.* **2006**, *30*, 102.

(39) Awati, P. S.; Awate, S. V.; Shah, P. P.; Ramasamy, V. Photocatalytic Decomposition of Methylene Blue Using Nanocrystalline Anatase Titania Prepared by Ultrasonic Technique. *Catal. Commun.* **2003**, *4*, 393.

(40) Srivastava, D. N.; Pol, V. G.; Palchik, O.; Zhang, L.; Yu, J. C.; Gedanken, A. Preparation of Stable Porous Nickel and Cobalt Oxides Using Simple Inorganic Precursor, Instead of Alkoxides, by a Sonochemical Technique. *Ultrason. Sonochem.* **2005**, *12*, 205.

(41) Yu, Y. C.; Zhang, L. Z.; Li, Q.; Kwong, K. W.; Xu, A. W.; Lin, J. Sonochemical Preparation of Nanoporous Composites of Titanium Oxide and Size-Tunable Strontium Titanate Crystals. *Langmuir* **2003**, *19*, 7673.

(42) Vollet, D. P.; Donatti, D. A.; Ruiz, A. I.; daSilva, J. S. P. About the Nanoporosity Elimination above 800 °C in Xerogels Prepared from TEOS Sono-Hydrolysis. *Phys. Stat. Sol. A, Appl. Res.* **2003**, *196*, 379.

(43) Liang, J. H.; Jiang, X.; Liu, G.; Deng, Z. X.; Zhuang, J.; Li, F. L. Characterization and Synthesis of Pure ZrO_2 Nanopowders via Sonochemical Method. *Mater. Res. Bull.* **2003**, *38*, 161.

(44) Kumar, V. G.; Aurbuch, D.; Gedanken, A. A Comparison between Hot-Hydrolysis and Sonolysis of Various Mn(II) Salts. *Ultrason. Sonochem.* **2003**, *10*, 17.

(45) Qian, D.; Jiang, J. Z.; Hansen, P. L. Preparation of ZnO Nanocrystals *via* Ultrasonic Irradiation. *Chem. Commun.* **2003**, 1078.

(46) Chave, T.; Nikitenko, S. I.; Granier, D.; Zemb, T. Sonochemical Reactions with Mesoporous Alumina. *Ultrason. Sonochem.* **2008**, *16*, 481.

(47) Sun, S. Q.; Li, T. Synthesis and Characterization of CdS Nanoparticles and Nanorods via Solvo-Hydrothermal Route. *Cryst. Growth. Des.* **2007**, *7*, 2367.

(48) Behboudnia, M.; Azizianekalandaragh, Y. Synthesis and Characterisation of CdSe Semiconductor Nanoparticles. *Mater. Sci. Eng., B* **2007**, *138*, 65.

(49) Behboudnia, M.; Khanbabaee, B. Conformational Study of CdS Nanoparticles Prepared by Ultrasonic Waves. *Colloid Surf. A* **2006**, *290*, 229.

(50) Liu, B.; Ren, T.; Zhang, J. R.; Chen, H. Y.; Zhu, J. J.; Burda, C. Spectroelectrochemistry of Hollow Spherical CdSe Quantum Dot Assemblies in Water. *Electrochem. Commun.* **2007**, *9*, 551.

(51) Thiruchitrambalam, M.; Palkar, V. R.; Gopinathan, V. Hydrolysis of Aluminium Metal and Sol-Gel Processing of Nano Alumina. *Mater. Lett.* **2004**, *58*, 3063.

(52) Bodisova, K.; Pach, L.; Kovar, V. The Influence of the Preferred Orientation of Boehmite Crystallites on α-Al_2O_3 Crystallization. *Ceram.-Silik.* **2005**, *49*, 34.

(53) Domingos, R. N.; Vollet, D. R.; Bucalon, A. J. Structural Changes Induced by Ultrasound During Aging of the Boehmite Phase. *Ultrason. Sonochem.* **1997**, *4*, 321.

(54) Chiche, D.; Digne, M.; Revel, R.; Chaneac, C.; Jolivet, J. P. Accurate Determination of Oxide Nanoparticle Size and Shape Based on X-Ray Powder Pattern Simulation: Application to Boehmite ALOOH. *J. Phys. Chem. C* **2008**, *112*, 8524.

(55) Mason, T. J. Ultrasound in Synthetic Organic Chemistry. *Chem. Soc. Rev.* **1997**, *26*, 443.

(56) Thompson, L. H.; Doraiswamy, L. K. Sonochemistry: Science and Engineering. *Ind. Eng. Chem. Res.* **1999**, *38*, 1215.

(57) Tettenhorst, R. T.; Hofmann, D. A. Crystal Chemistry of Boehmite. *Clays Clay Miner.* **1980**, *28*, 373.

(58) Tettenhorst, R. T.; Corbato, C. E. Comparison of Experimental and Calculated X-ray Powder Diffraction Data for Boehmite. *Clays Clay Miner.* **1988**, *36*, 181.

(59) Bellotto, M.; Rebours, B.; Euzen, P. Mechanism of Pseudo-boehmite Dehydration: Influence of Reagent Structure and Reaction Kinetics on the Transformation Sequence. *Mater. Sci. Forum* **1998**, *271*, 572.

(60) Reynolds, R. C., Jr. Effect of Particle Size on Apparent Lattice Spacings. *Acta Crystallogr., Sect. A* **1968**, *24*, 319.

(61) Mani, T. V.; Pillai, P. K.; Damodaran, A. D.; Warrier, K. G. K. Dependence of Calcination Conditions of Boehmite on the Alumina Particulate Characteristics and Sinterability. *Mater. Lett.* **1994**, *19*, 237.

(62) Tsukada, T.; Saito, T.; Segawa, H.; Yasumori, A.; Okada, K. Characterization of Pseudoboehmite and its Dispersibility in Nitric Acid Solution. *J. Ceram. Soc. Jpn.* **1999**, *107*, 359.

(63) Lippens, B. C.; Boer, J. H. D. Study of Phase Transformations during Calcination of Aluminum Hydroxides by Selected Area Electron Diffraction. *Acta Crystallogr.* **1964**, *17*, 1312.

(64) Guzman-Castillo, M. L.; Bokhimi, X.; Rodriguez-Hernandez, A.; Toledo-Antonio, A.; Hernandez-Beltran, F.; Fripiat, J. J. The Surface Energy of Quasi-amorphous γ-Alumina Calculated from the Temperature of the $\gamma \rightarrow \alpha$ Transition. *J. Non-Cryst. Solids* **2003**, *329*, 53.

(65) Buelna, G.; Lin, Y. S. Sol-Gel-Derived Mesoporous γ-Alumina Granules. *Microporous Mesoporous Mater.* **1999**, *30*, 359.

(66) Everett, D. H.; Stone, F. S. *The Structure and Properties of Porous Materials*; Butterworth: London, 1958.

(67) Jones, C. D.; Barron, A. R. Porosity, Crystal Phase, and Morphology of Nanoparticle Derived Alumina as a Function of the Nanoparticle's Carboxylate Substituent. *Mater. Chem. Phys.* **2007**, *104*, 460.

(68) Saha, B.; Ghoshal, A. K. Model-free Kinetics Analysis of Decomposition of Polypropylene over Al-MCM-41. *Thermochim. Acta* **2007**, *460*, 77.

(69) Sivasankar, T.; Paunikar, A. W.; Moholkar, V. S. Mechanistic Approach to Enhancement of the Yield of a Sonochemical. *Reaction. AIChE J.* **2007**, *53*, 1132.

Received for review November 24, 2009
Revised manuscript received March 26, 2010
Accepted April 11, 2010

IE901857Q